

# Merging binaries and magnetic white dwarfs

Gordon P. Briggs<sup>1</sup>, Lilia Ferrario<sup>1</sup>, Christopher A. Tout<sup>1,2,3</sup>,  
Dayal T. Wickramasinghe<sup>1</sup> and Jarrod R. Hurley<sup>4</sup>

<sup>1</sup>*Mathematical Sciences Institute, The Australian National University, ACT 0200, Australia*

<sup>2</sup>*Institute of Astronomy, The Observatories, Madingley Road, Cambridge CB3 0HA, UK*

<sup>3</sup>*Monash Centre for Astrophysics (MoCA), School of Mathematical Sciences, Monash University, VIC 3800, Australia*

<sup>4</sup>*Centre for Astrophysics & Supercomputing, Swinburne University of Technology, Hawthorn, VIC 3122, Australia*

Accepted. Received ; in original form

## ABSTRACT

A magnetic dynamo driven by differential rotation generated when stars merge can explain strong fields in certain classes of magnetic stars, including the high field magnetic white dwarfs (HFMWDs). In their case the site of the differential rotation has been variously proposed to be within a common envelope, the massive hot outer regions of a merged degenerate core or an accretion disc formed by a tidally disrupted companion that is subsequently incorporated into a degenerate core. We synthesize a population of binary systems to investigate the stellar merging hypothesis for observed single HFMWDs. Our calculations provide mass distribution and the fractions of white dwarfs that merge during a common envelope phase or as double degenerate systems in a post common envelope phase. We vary the common envelope efficiency parameter  $\alpha$  and compare with observations. We find that this hypothesis can explain both the observed incidence of magnetism and the mass distribution of HFMWDs for a wide range of  $\alpha$ . In this model, the majority of the HFMWDs are of the Carbon Oxygen type and merge within a common envelope. Less than about a quarter of a per cent of HFMWDs originate from double degenerate stars that merge after common envelope evolution and these populate the high-mass tail of the HFMWD mass distribution.

**Key words:** white dwarfs – magnetic fields – binaries: general – stars: evolution

## 1 INTRODUCTION

Magnetic fields are seen in main-sequence stars of most spectral types. They are usually considered to be either of fossil origin, arising from a conserved primordial field, or generated in a contemporary dynamo (Mestel & Landstreet 2005). The latter is the accepted explanation for magnetic stars with convective envelopes such as the low-mass ( $M < 1.5 M_{\odot}$ ) main-sequence stars. The origin of the fields in the higher-mass magnetic Ap and Bp main-sequence stars with radiative envelopes is less certain. While a fossil origin remains possible, it has been proposed that magnetic fields may be generated by a dynamo mechanism driven by various instabilities, including the magnetorotational instability, in differentially rotating radiative regions of single stars (see e.g. Potter, Chitre & Tout 2012).

The origin of the high field magnetic white dwarfs (HFMWDs) has been the topic of much discussion in recent years. The incidence of magnetism in white dwarfs in the high field group ( $B > 10^6$  G) is estimated to be about 8–16 per cent (Liebert, Bergeron & Holberg 2003; Kawka et al. 2007). A traditional explanation has been that the fields are of a fossil origin from the main sequence with magnetic

flux conserved in some way during evolution to the white dwarf phase (Mestel & Landstreet 2005). Kawka et al. (2007) pointed out that the strongly magnetic Ap and Bp stars could not be their sole progenitors because the birth rate of these main-sequence stars is insufficient to explain the observed birth rate of the HFMWDs. However this turned out not to be a strong argument against the fossil hypothesis. In an earlier paper Wickramasinghe & Ferrario (2005) noted that it could be reconciled if about 40 per cent of late B stars had fields below the observed threshold for Ap and Bp stars. This would be consistent with the observations of Power et al. (2008) who conducted a volume-limited study of the magnetic Ap and Bp stars within 100 pc of the Sun. Their study has shown that the incidence of magnetism in intermediate mass stars increases with the mass of the stars. At  $1.7 M_{\odot}$  the fraction of magnetic among non-magnetic stars is only 0.1 per cent, while at  $3.5 M_{\odot}$  it is 37.5 per cent.

Some 50 per cent of stars are in binary systems. As these evolve some can interact and merge. So we may expect that some stars that appear single today are the result of the merging of two stars. The possibility of generating strong magnetic fields during such merging events has often been

arXiv:1412.5662v1 [astro-ph.SR] 17 Dec 2014

discussed in the literature as an alternative explanation for magnetic fields in certain classes of stellar object. Indeed, as an alternative to the fossil field model, Ferrario et al. (2009) proposed that the strong fields in the magnetic A, B and O stars are generated as stars merge.

Here we focus on the hypothesis that the entire class of HFMDs with fields  $10^6 < B/G < 10^9$  owe their magnetic fields to merging (Tout et al. 2008). This model was first devised to explain the observation that there are no examples of HFMDs in wide binary systems with late-type companions while a high fraction of non-magnetic white dwarfs are found in such systems (Liebert et al. 2005).

In the common envelope scenario, when a giant star fills its Roche lobe, unstable mass transfer can lead to a state in which the giant's envelope engulfs both cores. As the two cores spiral together, energy and angular momentum are transferred from their orbit to the differentially rotating common envelope until it is ejected, leaving behind a close binary system, or a merged single object. In the original model for formation of HFMDs Tout et al. (2008) envisaged that the fields are generated by a dynamo in the common envelope and diffuse into the partially degenerate outer layers of the proto-white dwarf before the common envelope is ejected. If the end product is a single star it can have a highly magnetic core and if it is a very close binary, it can become a magnetic cataclysmic variable. Potter & Tout (2010) attempted to model this phenomenon and found a potential problem in that the time-scale for the diffusion of the field into the white dwarf is generally significantly longer than the expected common envelope lifetime.

Wickramasinghe, Tout & Ferrario (2014) suggested that strong magnetic fields in white dwarfs are generated by a dynamo process that feeds on the differential rotation in the merged object as it forms. A weak poloidal seed field that is already present in the pre-white dwarf core is amplified by the dynamo to a strong field that is independent of its initial strength but depends on the amount of the initial differential rotation. We note in this context that weak fields of  $B \leq 1$  kG may be present in most white dwarfs (Landstreet et al. 2012). Presumably these can be generated in a core-envelope dynamo in the normal course of stellar evolution.

Nordhaus et al. (2011) proposed an alternative but similar model (hereinafter the disc field model). They noted that if the companion were of sufficiently low mass it would be disrupted while merging and form a massive accretion disc around the proto-white dwarf. Fields generated in the disc via the magnetorotational instability or other hydrodynamical instabilities could then be advected on to the surface of the proto-white dwarf and so form a HFMD. Such a model could apply to some merging cores within the common envelope, depending on component masses, and to post-common envelope merging double degenerate systems (DDs). It depends on the time-scale for the diffusion of the field into the white dwarf envelope.

García-Berro et al. (2012) used the results of a three-dimensional hydrodynamic simulation of merging DDs to argue that a massive hot and differentially rotating convective corona forms around the more massive component and used equipartition arguments to estimate that fields of about  $3 \times 10^{10}$  G could be generated. They also presented a population synthesis study of white dwarfs that formed specifically as merging DDs, assuming a common envelope

energy efficiency parameter  $\alpha = 0.25$ , and showed that there is general agreement with the observed properties of high-mass white dwarfs ( $M_{\text{WD}} > 0.8 M_{\odot}$ ) and HFMDs. However they did not consider merging when the companion is a non-degenerate star.

We hypothesize that single white dwarfs that demonstrate a strong magnetic field are the result of merging events, so we carry out a comprehensive population synthesis study of merging binary systems for different common envelope efficiencies  $\alpha$ . We consider all possible routes that could lead to a single white dwarf. We isolate the white dwarfs formed by the merging of two degenerate cores, either as white dwarfs, a red giant plus a white dwarf or two red giants, from those formed by a giant merging with a main-sequence star and show that the observed properties of the HFMDs are generally consistent with the common envelope hypothesis for  $0.1 \leq \alpha \leq 0.3$ . Both groups contribute to the observed distribution but main-sequence companions merging with degenerate cores of giants form most of the HFMDs.

## 2 COMMON ENVELOPE EVOLUTION AND FORMULISM

When one of the stars in a binary system becomes a giant, it expands and overfills its Roche lobe. Mass transfer soon proceeds typically, but not always, on a dynamical time-scale (Han et al. 2002). The giant envelope rapidly engulfs both the companion star and the core of the donor to form a common envelope. The two dense cores, that of the giant and the accreting star itself, interact with the envelope, transferring to it orbital energy and angular momentum. The envelope can be partly or wholly ejected and the orbit of the engulfed star shrinks. It is not known how long this process takes but it is generally thought to last for more of a dynamical stellar time-scale than a thermal or nuclear time-scale. It probably has never been observed. If the companion succeeds in fully ejecting the envelope the two cores survive in a binary system with a much smaller separation. If the envelope is not fully ejected the orbit may completely decay and the two stars coalesce. When the envelope of a giant engulfs a degenerate companion the two cores can merge but if the companion is non-degenerate it either merges with the envelope or accretes on to the giant core. When the initial masses of the two stars are within a few percent both can expand to giants at the same time and Roche lobe overflow (RLOF) leads to a double common envelope.

The common envelope process was first proposed to explain binary star systems, such as cataclysmic variables (CVs), whose orbital separations are smaller than the original radius of the progenitor primary star. A mechanism was needed to explain how this could occur. The possible existence of common envelopes was first proposed by Bisnovaty-Kogan & Sunyaev (1971). Its qualitative description is based on evolutionary necessity rather than mathematical physics. While it is sufficient to explain a variety of exotic stars and binaries that could not otherwise be explained, a full mathematical model has yet to be developed to describe the interaction in detail and to test the various theories.

A simple quantitative model of common envelope evolution is the energy or  $\alpha$  formulism (van den Heuvel 1976). For

this the change in orbital energy  $\Delta E_{\text{orb}}$  of the in-spiralling cores is equated to the energy required to eject the envelope to infinity, the binding energy  $E_{\text{bind}}$ . The total orbital energy, kinetic plus potential, of a binary star with masses  $m_1$  and  $m_2$  and separation  $a$  is  $E_{\text{orb}} = -Gm_1m_2/2a$ . However the envelope ejection cannot be completely efficient so Livio & Soker (1988) introduced an efficiency parameter  $\alpha$  to allow for the fraction of the orbital energy actually used to eject the envelope.

$$\Delta E_{\text{orb}} = \alpha E_{\text{bind}}. \quad (1)$$

Following Tauris & Dewi (2001) we use a form of the binding energy that depends on the detailed structure of the giant envelope and adopt

$$E_{\text{bind}} = -\frac{Gm_1m_{1,\text{env}}}{\lambda R_1}, \quad (2)$$

where  $R_1$  is the radius of the primary envelope. The constant  $\lambda$  was introduced by de Kool (1990) to characterize the envelope structure. Our  $\lambda$  depends on the structure of the particular star under consideration. It is sensitive to how the inner boundary between the envelope and the remnant core is identified (Tauris & Dewi 2001) and includes the contributions from the thermal energy of the envelope on the assumption that it remains in equilibrium as it is ejected.

The initial orbital energy is that of the secondary star  $m_2$  and the primary core  $m_{1,c}$  at the orbital separation  $a_i$  at the beginning of common envelope and is given by

$$E_{\text{orb},i} = -\frac{1}{2} \frac{Gm_{1,c}m_2}{a_i} \quad (3)$$

and the final orbital energy is

$$E_{\text{orb},f} = -\frac{1}{2} \frac{Gm_{1,c}m_2}{a_f}, \quad (4)$$

where  $a_f$  is the final orbital separation. Thus we have

$$\Delta E_{\text{orb}} = E_{\text{orb},f} - E_{\text{orb},i}. \quad (5)$$

From this we can calculate  $a_f$  which is the separation of the new binary if the cores do not merge. If  $a_f$  is so small that either core would overflow its new Roche lobe, then the cores are considered to merge when  $a_f$  is such that the core just fills its Roche lobe. Setting  $a_f$  to this separation we calculate  $E_{\text{orb},f}$  and  $\Delta E_{\text{orb}}$  with equations 4 and 5. Then we calculate a final binding energy for the envelope around the merged core

$$E_{\text{bind},f} = E_{\text{bind},i} + \frac{\Delta E_{\text{orb}}}{\alpha}. \quad (6)$$

Assuming this envelope has a normal giant structure  $R(m, m_c)$  we calculate how much mass must be lost. In the case of a double common envelope, the initial orbital energy is that of both cores and the binding energies of the two envelopes added.

Some difficulties with the energy formulation arise because  $\alpha$  can depend on the duration of the common envelope phase. If it lasts longer than a nuclear or thermal time-scale then alterations in the envelope, owing to adjustments in its thermal equilibrium, can change its structure and hence  $\lambda$ . Changes to the energy output from the core, owing to the decreasing weight of the diminishing envelope, can also affect the thermal equilibrium and thence  $\lambda$ . We do not consider these complications in this work. Nor do we include ionization and dissociation energy, as proposed by Han et al. (1994) in the envelope binding energy.

**Table 1.** Stellar types distinguished within the BSE algorithms.

Type	Description
0.	Deep or fully convective low-mass MS star (CS)
1.	Main-sequence star (MS)
2.	Hertzsprung gap star (HG)
3.	First giant branch (RGB)
4.	Core helium Burning
5.	First asymptotic giant branch (early AGB)
6.	Second asymptotic giant branch (late AGB)
7.	Main-sequence naked helium star
8.	Hertzsprung gap naked helium star
9.	Giant branch naked helium star
10.	Helium white dwarf (He white dwarf)
11.	Carbon/oxygen white dwarf (CO white dwarf)
12.	Oxygen/neon white dwarf (ONe white dwarf)
13.	Neutron star
14.	Black hole
15.	Massless supernova/remnant

### 3 POPULATION SYNTHESIS CALCULATIONS

We evolve synthetic populations of binary star systems from the zero-age main sequence (ZAMS). Each system requires three initial parameters, the primary star mass, the secondary star mass and the orbital period. The primary masses  $M_1$  are allocated between 0.8 and 12.0  $M_{\odot}$  and the secondary star masses  $M_2$  between 0.1 and 12.0  $M_{\odot}$ . The binary orbits are specified by a period  $P_0$  at ZAMS between 0.1 and 10 000 d and zero eccentricity. Each parameter was uniformly sampled on a logarithmic scale for 200 divisions. This scheme gives a synthetic population of some 6 million binary systems. We calculate the effective number of actual binary systems by assuming that the primary stars are distributed according to Salpeter's mass function (Salpeter 1955)  $N(M) dM \propto M^{-2.35} dM$ , where  $N(M) dM$  is the number of stars with masses between  $M$  and  $M + dM$ , and that the secondary stars follow a flat mass ratio distribution for  $q \leq 1$  (e.g. Ferrario 2012). The initial period distribution was taken to be logarithmically uniform in the range  $-1 \leq \log_{10} P_0/d \leq 4$ .

Each binary system was evolved from the ZAMS to an age of 9.5 Gyr, taken to be the age of the Galactic disc (e.g. Oswalt et al. 1996; Liu & Chaboyer 2000), with the rapid binary star evolution (BSE) algorithm developed by Hurley, Tout & Pols (2002). This is an extension of their single star evolution algorithm (Hurley, Pols & Tout 2000) in which they use analytical formulae to approximate the full numerical hydrodynamic and nuclear evolution of stars. This includes mass-loss episodes during various stages of evolution. The BSE code adds interactions between stars, such as mass transfer, RLOF, common envelope evolution, supernova kicks and angular momentum loss by gravitational radiation and magnetic braking as well as tidal interaction. We summarize the type of stars that play a role in the BSE code in Table 1.

In the BSE model we use the  $\alpha$  (energy) formulism for common envelope phases and have taken a fixed  $\lambda = 0.5$  as representative of the range expected for our stars. We take  $\alpha$  to be a free parameter between 0.1 and 0.9. Efficiencies of  $\alpha > 1$  are only possible if additional energy sources

**Table 2.** Fraction of binary systems that merge during common envelope for various values of  $\alpha$ . The fraction of white dwarfs born from merged stars in a single generation of binary systems of age 9.5 Gyr (the age of the Galactic disc) is  $N$ . The remaining six columns give the smallest and the largest parameters on the search grid for systems that are found to have merged. The parameters are the progenitors’ ZAMS masses and orbital period.

$\alpha$	$N$ per cent	$M_{1\min}/M_{\odot}$	$M_{2\min}/M_{\odot}$	$P_{0\min}/\text{d}$	$M_{1\max}/M_{\odot}$	$M_{2\max}/M_{\odot}$	$P_{0\max}/\text{d}$
0.05	11.58	1.08	0.10	348.9	11.06	2.77	16.3
0.10	10.35	1.08	0.10	195.6	11.06	2.90	20.5
0.20	8.86	1.08	0.10	97.7	11.21	2.77	20.5
0.25	8.17	1.08	0.10	82.1	11.21	4.06	932.9
0.30	7.55	1.08	0.10	65.2	11.21	4.06	784.3
0.40	6.51	1.08	0.10	48.8	11.21	4.06	587.3
0.50	5.70	1.08	0.10	38.7	11.21	4.06	493.7
0.60	5.06	1.08	0.10	30.7	11.21	4.06	391.7
0.70	4.60	1.08	0.10	25.8	11.21	3.87	195.6
0.80	4.18	1.08	0.10	23.7	11.21	3.12	82.1
0.90	3.75	1.08	0.10	19.3	11.06	4.06	415.0

**Table 3.** Fraction of merging DD systems, white dwarfs formed by merging of two degenerate objects outside a common envelope in a single generation of binary systems of age 9.5 Gyr. Other columns are as in Table 2

$\alpha$	$N$ per cent	$M_{1\min}/M_{\odot}$	$M_{2\min}/M_{\odot}$	$P_{0\min}/\text{d}$	$M_{1\max}/M_{\odot}$	$M_{2\max}/M_{\odot}$	$P_{0\max}/\text{d}$
0.05	$4.49 \times 10^{-5}$	2.41	1.79	1867.9	4.21	2.17	3331.3
0.10	$4.89 \times 10^{-4}$	2.02	1.79	1245.9	4.21	2.28	2097.0
0.20	$1.01 \times 10^{-4}$	1.99	1.98	932.9	4.21	2.28	1867.9
0.25	$1.29 \times 10^{-4}$	1.99	1.98	784.3	4.21	2.28	1867.9
0.30	$1.69 \times 10^{-4}$	1.52	1.52	587.3	4.27	2.23	1867.9
0.40	$2.62 \times 10^{-4}$	1.52	1.52	587.3	4.21	2.34	1663.8
0.50	$3.42 \times 10^{-4}$	1.52	1.52	587.3	4.27	2.28	1570.3
0.60	$4.07 \times 10^{-4}$	1.52	1.52	587.3	6.24	1.59	12.2
0.70	$4.36 \times 10^{-4}$	1.52	1.52	587.3	6.33	1.59	11.5
0.80	$4.11 \times 10^{-4}$	1.54	1.52	587.3	6.59	1.71	10.2
0.90	$3.74 \times 10^{-4}$	1.54	1.52	587.3	6.42	1.71	9.7

are involved in the process. We do not consider this here. We use the full suite of mass-loss rates described by Hurley, Pols & Tout (2000). We found that, in order to generate sufficient low-mass white dwarfs,  $\eta = 1.0$  for Reimers’ mass-loss parameter is necessary so we have used this throughout. Alternatively sufficient low-mass white dwarfs could be formed with smaller  $\eta$  if the Galactic disc were somewhat older. Meng et al. (2008) produce them with  $\eta = 0.25$  in populations of 12 Gyr in age. The metallicity is taken to be solar ( $Z = 0.02$ ) in all our calculations.

From all evolved systems we select those that could generate single HFWDs. To this end we select all pairs of white dwarfs that merge outside any common envelope and leave a single white dwarf remnant. These are our white dwarf-white dwarf (DD) mergers. Added to these are white dwarf remnants of systems that underwent at least one common envelope phase and merged during the last common envelope phase and satisfy two further criteria. Firstly, either one or both of the stars must have a degenerate core before merging and secondly, there must be no further core burning before the remnant white dwarf is exposed. We assume that such a core burning would be convective and destroy any frozen-in high magnetic field.

## 4 POPULATION SYNTHESIS RESULTS

Assuming a constant star formation rate, each synthetic population was integrated to the Galactic disc age over the entire parameter space with  $0.05 \leq \alpha \leq 0.9$ . Table 2 lists the fraction by type of all binary systems that merge in a common envelope and Table 3 those that merge as DDs in a single generation of stars of age 9.5 Gyr. The tables also show the limits of the parameter space within which the cores merge. The minimum ZAMS masses of the systems that merged and ended their lives as single white dwarfs are listed in the columns  $M_{1\min}$  and  $M_{2\min}$  and the minimum initial period in the column  $P_{0\min}$ . The maximum ZAMS masses and period are shown in the columns  $M_{1\max}$ ,  $M_{2\max}$  and  $P_{0\max}$ . For systems that merge during a common envelope phase the minimum ZAMS primary mass is determined by the age of the Galactic disc and thus by the time taken by this star to evolve off the main sequence. For the DD route both stars must evolve to white dwarfs. After the last common envelope episode, the two stars continue their evolution to the white dwarf final stage. The stars are then brought together by gravitational radiation and eventually coalesce. This process takes longer than the common envelope route. As a consequence, the main-sequence evolution lifetime of the primary star must be shorter and thus the minimum ZAMS mass must be larger than that required to merge during common envelope evolution. Otherwise such

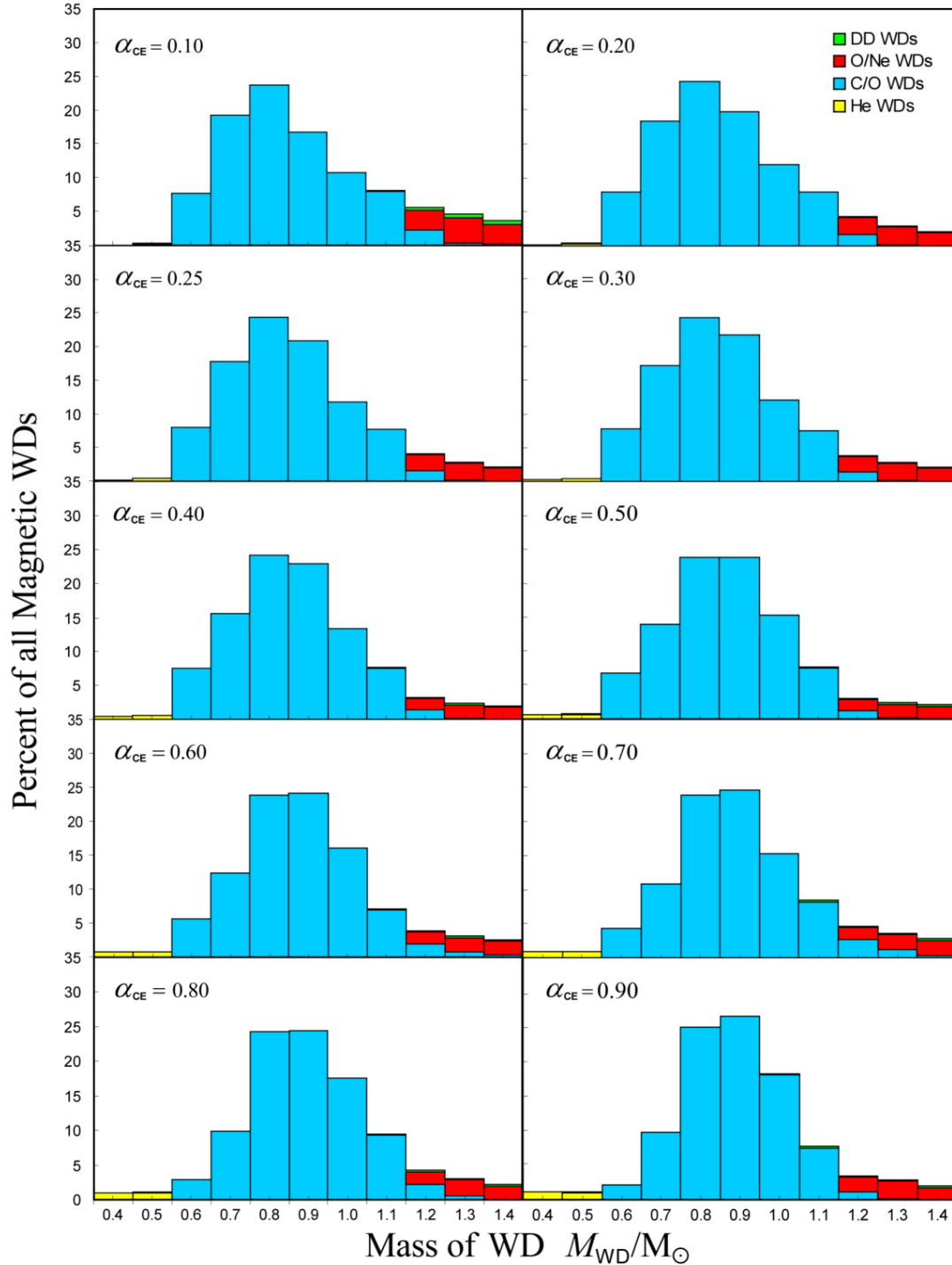


**Figure 1.** Theoretical mass distribution of remnant white dwarfs formed by merging for a range of values  $\alpha$  and a Galactic disc age of 9.5 Gyr. ‘DD white dwarfs’ are white dwarfs resulting from DD mergers, ‘O/Ne white dwarfs’ are Oxygen-Neon white dwarfs, ‘CO white dwarfs’ are Carbon-Oxygen white dwarfs and ‘He white dwarfs’ are helium white dwarf remnants after merging. This figure will appear in colour in the on-line version of this paper making it clearer as to what are the components of the high mass tail of the distribution.

**Table 4.** Types and fractions per cent of white dwarfs formed from common envelope and DD by merging binary systems in a population aged 9.5 Gyr. All DD white dwarfs are of CO type.

$\alpha$	Common envelope			Double degenerate
	He	CO	ONe	CO
0.05	0.04	88.77	11.04	0.15
0.10	0.16	88.73	9.79	1.32
0.20	0.43	92.14	7.08	0.36
0.25	0.55	92.24	6.74	0.47
0.30	0.68	92.10	6.63	0.58
0.40	0.94	92.89	5.42	0.75
0.50	1.20	92.55	5.41	0.84
0.60	1.45	91.70	5.95	0.89
0.70	1.68	91.20	6.27	0.85
0.80	1.92	91.12	6.12	0.84
0.90	2.20	90.42	6.47	0.91

systems would not be able to coalesce within the age of the Galactic disc.

For low values of  $\alpha$  the envelope clearance efficiency is low and the time for the envelope to exert a drag force on the orbit is largest. Correspondingly, Table 2 shows that, for low  $\alpha$ , the number of coalescing stars in the common envelope path is maximal. As  $\alpha$  increases, the time for ejection of the envelope decreases and the number of systems that merge while still in the common envelope also decreases. White dwarfs formed from merged stars are of the three types He, CO and ONe. The small fraction of He white dwarfs increases with  $\alpha$  while that of the ONe white dwarfs falls. The He white dwarfs originate when RGB stars coalesce with very low-mass main-sequence stars. At low  $\alpha$  these stars merge when there is very little envelope left and the resulting giant can lose the rest of its envelope before helium ignition. As  $\alpha$  is increased, more of the envelope remains after coalescence and the stars pass through core helium burning before being exposed as CO white dwarfs. The ONe white dwarfs form when the most evolved AGB stars coalesce with their companions. These stars have only rather weakly bound envelopes so that as  $\alpha$  is increased more of them emerge from the common envelope phase detached. For the DD case we find that only CO white dwarfs are formed in our models. Table 4 sets out the types and fractions of all white dwarfs that form from common envelope and DD merging systems as a function of  $\alpha$ . The lack of merged He white dwarfs seems to indicate that, while it is true that very low-mass white dwarfs ( $M \lesssim 0.4 M_{\odot}$ ) must arise from binary interaction, they do not arise from DD mergers within a Galactic disc age of 9.5 Gyr.

#### 4.1 Example evolutionary histories

The precise evolutionary history of a binary system depends on its particular parameters. For example the number of common envelope events that can occur can vary from one to several (Hurley, Tout & Pols 2002). Here we give a few examples to illustrate the difference between common envelope and DD merging events.

##### 4.1.1 Common envelope coalescence

Table 5 sets out the evolutionary history of an example system that merges during a common envelope with  $\alpha = 0.2$ . The progenitors are a primary star S1 of  $4.44 M_{\odot}$  and a secondary S2 of sub-solar mass  $0.72 M_{\odot}$ . At ZAMS the initial period is 219.6 d and the orbit is circular with a separation of  $264.7 R_{\odot}$ . S1 evolves first and reaches the early AGB at 161.77 Myr having lost  $0.02 M_{\odot}$  on the way. Roche lobe overflow starts 0.2 Myr later with mass flowing from S1 to S2. At this point the orbital separation has decreased to  $141.4 R_{\odot}$  because orbital angular momentum has been lost through tidal spin up of S1. A common envelope develops and the two cores coalesce when their separation reaches  $0.53 R_{\odot}$ . A further  $0.6 M_{\odot}$  of the envelope has been lost. At 162.78 Myr, approximately 0.9 Myr after coalescing, S1 becomes a late stage AGB star. After a further 0.7 Myr it becomes a CO white dwarf.

##### 4.1.2 DD coalescence

In the DD pathway both stars survive the common envelope without merging and both continue to evolve to white dwarfs approaching each other through gravitational radiation to eventually coalesce. Table 6 illustrates this for  $\alpha = 0.1$ . At ZAMS the progenitors are a  $3.7 M_{\odot}$  primary and a  $1.9 M_{\odot}$  secondary with an initial period of 3444 d and a separation of  $1603 R_{\odot}$ , again in a circular orbit. The primary evolves through to a late stage AGB star after 270.5 Myr losing  $0.6 M_{\odot}$  on the way. The separation falls to  $1509 R_{\odot}$ . As a late AGB star S1 loses  $0.9 M_{\odot}$  of which  $0.02 M_{\odot}$  is accreted by S2 from the wind. Approximately 0.5 Myr later, at 271 Myr with S1 of mass  $2.68 M_{\odot}$  and S2  $1.95 M_{\odot}$ , RLOF commences and a common envelope develops. The orbital separation falls to  $374 R_{\odot}$  when the envelope is ejected. S2 continues to evolve, first as a blue straggler then through the Hertzsprung gap, red giant and core helium burning stages until it becomes an early AGB star at 1513.4 Myr. At 1517.3 Myr RLOF begins again and a second common envelope forms. At an orbital separation of only  $2.43 R_{\odot}$  the envelope is ejected and S2 emerges as a CO white dwarf of mass  $0.54 M_{\odot}$ . A long period of orbital contraction by gravitational radiation follows until at 9120.8 Myr the two white dwarfs are separated by  $0.04 R_{\odot}$  and RLOF from S2 to S1 begins followed rapidly by coalescence of the DDs. The remnant star is still a CO white dwarf but now of mass  $1.36 M_{\odot}$ .

#### 4.2 Mass distribution of the synthetic population

With the selected common envelope and DD merged systems we generate a population of putative magnetic white dwarfs by integration over time from  $t = 0$  to 9.5 Gyr, our chosen age for the Galactic disc. The star formation rate is taken to be constant over the lifetime of the Galactic disc. Whereas Tables 2 and 3 show the relative numbers of merged white dwarfs from a single generation of binary stars, continuous star formation over the lifetime of the Galaxy builds up a population of white dwarfs that favours higher-mass systems because at lower-mass, especially in later generations, they do not have enough time to evolve. Similarly, the slow orbital contraction by gravitational radiation means that potential DD coalescence in later generations is not complete

**Table 5.** Evolutionary history of an example binary system that merges during common envelope. Here  $\alpha = 0.2$ ,  $P_0 = 219.6$  d, S1 is the primary star and S2 is the secondary star.

Stage	Time/Myr	$M_1/M_\odot$	$M_2/M_\odot$	$a/R_\odot$	Remarks
1	0.0000	4.444	0.719	264.679	ZAMS
2	138.1295	4.444	0.719	264.679	S1 becomes a Hertzsprung gap star
3	138.7479	4.444	0.719	264.739	S1 becomes a red giant
4	139.1676	4.443	0.719	179.877	S1 starts core helium burning. Some mass loss occurs
5	161.7637	4.402	0.719	181.495	S1 first AGB
6	161.9691	4.402	0.719	141.380	S1 begins RLOF
7	161.9691	4.524	-	0.529	common envelope: S1, S2 coalesce; RLOF ends
8	162.8725	4.494	-	-	S1 becomes late AGB
9	163.5543	0.924	-	-	S1 becomes CO white dwarf

**Table 6.** Evolutionary history of an example of white dwarf that formed in a double degenerate coalescence. Here  $\alpha = 0.1$ ,  $P_0 = 3144$  days, S1 is the primary star and S2 the secondary star.

Stage	Time/Myr	$M_1/M_\odot$	$M_2/M_\odot$	$a/R_\odot$	Remarks
1	0.0000	3.673	1.928	1603.362	ZAMS
2	222.4734	3.673	1.928	1603.362	S1 becomes a Hertzsprung gap star
3	223.6164	3.673	1.928	1603.416	S1 becomes a Red Giant
4	224.6021	3.672	1.928	1603.678	S1 starts core helium burning
5	268.5530	3.645	1.928	1611.505	S1 becomes early AGB
6	270.4541	3.614	1.928	1583.219	S1 becomes late AGB
7	270.9681	2.682	1.947	1509.115	S1 begins RLOF, mass transfer on to S2 and mass loss occurs
8	270.9681	0.821	1.947	374.233	common envelope. S1 emerges as a CO white dwarf and RLOF ends
9	1260.0681	0.821	1.947	374.233	Begin Blue Straggler phase
10	1267.0548	0.821	1.947	374.233	S2 becomes a Hertzsprung gap star
11	1277.4509	0.821	1.946	374.245	S2 becomes a Red Giant
12	1306.9423	0.821	1.943	375.353	S2 starts core helium burning
13	1513.3615	0.821	1.926	377.768	S2 becomes early AGB
14	1517.2953	0.821	1.913	324.600	S2 begins Roche lobe overflow
15	1517.2953	0.821	0.536	2.433	common envelope begins. S2 evolves to a CO white dwarf and RLOF ends
16	9120.8467	0.821	0.536	0.040	S2 begins RLOF
17	9120.8467	1.357	-	0.000	S1, S2 coalesce

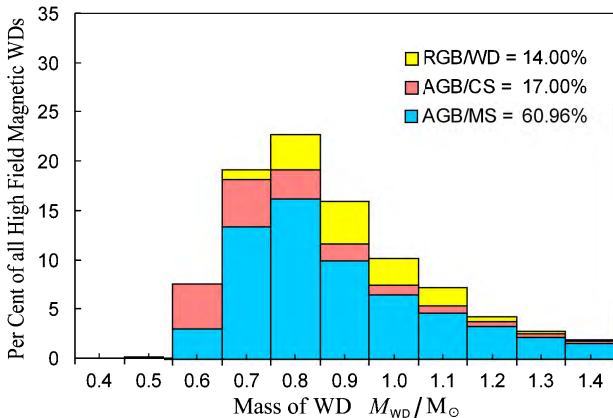


**Figure 2.** Mass distribution of theoretical HFMWDs for  $\alpha = 0.10$  separated according to their pre-common envelope progenitors. Other paths also contribute but are less than 1 per cent of the total. The Galactic disc age is chosen to be 9.5 Gyr. The stellar types are identified in Table 1. This figure will appear in colour in the on-line version of this paper making it clearer as to what are the various paths.

and the fraction of those white dwarfs is further reduced in the present day population. Fig. 1 shows the mass distri-

bution for CO, ONe and DD white dwarfs in a present day population formed over the age of the Galactic disc, 9.5 Gyr. Fig. 2 shows the contributions from the various pre-common envelope progenitor pairs that formed the post-common envelope white dwarfs either through the common envelope or DD path when  $\alpha = 0.1$ . Other paths also contribute but to less than 3 per cent of the total each. Table 7 lists their contributions summed over all white dwarf masses.

In order to calculate the incidence of HFMWDs we used the same BSE code to model single star evolution through to the white dwarf stage also for a Galactic disc age of 9.5 Gyr under the assumption that all white dwarfs originating from single star evolution are non-magnetic. Table 8 sets out the incidence of HFMWDs as a percentage of the incidence of field white dwarfs for a range of  $\alpha$ .

## 5 COMPARISON WITH OBSERVATIONS

We compare our theoretical predictions with observations of HFMWDs. Our comparison includes (i) the incidence of magnetism among single white dwarfs and (ii) the mass distribution of single HFMWDs. This is not a simple task because the observational data base of HFMWDs is a mixed bag of objects from many different ground and space-borne

**Table 7.** The contributions per cent of pre-common envelope progenitor pairs to theoretical HFMWDs when  $\alpha = 0.1$ . The stellar type ‘CS’ is a deeply or fully convective low-mass main sequence star (see Table 1).

Progenitor pairs	Fraction per cent
AGB/MS	60.96
AGB/CS	17.00
RGB/CO WD	14.00
AGB/HG	2.72
AGB/CO WD	2.21
CO WD/CO WD	1.32
RGB/RGB	0.97
RGB/AGB	0.46
RGB/CS	0.16
AGB/AGB	0.20

**Table 8.** The theoretical incidence of HFMWDs as a fraction of magnetic to non-magnetic field white dwarfs as a function of the common envelope efficiency parameter  $\alpha$ .

$\alpha$	HFMWDs per cent		
	CE	DD	Total
0.05	21.63	$3.16 \times 10^{-2}$	21.67
0.10	18.99	$2.58 \times 10^{-1}$	19.25
0.20	16.12	$5.80 \times 10^{-1}$	16.18
0.25	14.78	$7.02 \times 10^{-2}$	14.85
0.30	13.50	$8.03 \times 10^{-2}$	13.58
0.40	11.85	$8.80 \times 10^{-2}$	11.67
0.50	10.10	$8.64 \times 10^{-2}$	10.18
0.60	8.94	$8.11 \times 10^{-2}$	9.02
0.70	8.15	$7.01 \times 10^{-2}$	8.22
0.80	18.99	$6.33 \times 10^{-2}$	7.50
0.90	18.99	$6.24 \times 10^{-2}$	6.78

surveys. It is plagued by observational biases. In magnitude-limited surveys, such as the Palomar-Green (PG) or the Hamburg-Schmidt surveys, one of the biases against the detection of magnetic white dwarfs has been that since these are generally more massive than their non-magnetic counterparts (Liebert 1988), their radii are smaller and therefore they are less luminous. Similar biases would also apply to UV and X-ray surveys. However Liebert, Bergeron & Holberg (2003) have argued that, in any *explicitly magnitude-limited survey*, it may be possible to correct for the difference in search volume for the magnetic white dwarfs. Thus a re-analysis of the data of the PG survey, that took into account the different volumes that are sampled by different mass white dwarfs, gave an estimate for the fraction of HFMWDs of at least  $7.9 \pm 3$  per cent (Liebert, Bergeron & Holberg 2003). Volume-limited samples are expected to be less affected by the radius bias but contain very few magnetic white dwarfs with known masses or temperatures. A nearly complete volume-limited sample of nearby white dwarfs by Kawka et al. (2007) shows that up to  $21 \pm 8$  per cent of all white dwarfs within 13 pc have magnetic fields greater than about 3 kG and  $11 \pm 5$  per cent are HFMWDs with  $B \geq 1$  MG.

The synthetic population generated by BSE is a volume-limited sample and so is not directly comparable with a magnitude limited sample such as the Sloan Digital Sky Survey

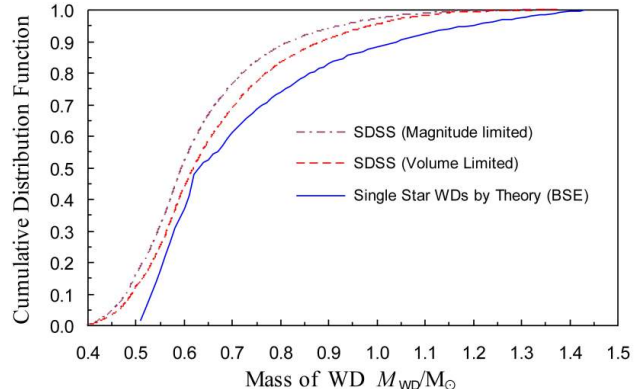


**Figure 3.** CDFs of masses of observed SDSS DR7 (Kleinman et al. 2013) non-magnetic, magnitude-limited and converted-volume-limited field white dwarfs and the theoretical (BSE) volume-limited population of non-magnetic white dwarfs from single star evolution for a Galactic disc age of 9.5 Gyr.

Data Release 7 (SDSS DR7) white dwarf catalogue (Kleinman et al. 2013) which has 12 803 members. Liebert, Bergeron & Holberg (2003) estimated that the limiting distance to which a white dwarf can be found in a magnitude-limited survey is proportional to its radius  $R_{WD}$ . Thus the survey volume for a given mass scales as  $R_{WD}^3$ . We correct this bias by weighting each white dwarf found by the SDSS in proportion to  $1.0/R_{WD}^3$  relative to the radius of a  $0.8 M_{\odot}$  white dwarf. The cumulative distribution function (CDF) for the corrected mass distribution along with the CDF for the uncorrected mass distribution of the SDSS white dwarfs is shown in Fig. 3. The theoretical CDF obtained with BSE for the mass distribution of single white dwarfs is shown for comparison.

We note that the BSE code we use does not produce low-mass white dwarfs because of the limited age of our Galactic disc. However Han et al. (1994) and Meng et al. (2008) have constructed single star models using different assumptions utilizing a superwind that produces low-mass white dwarfs in older populations. This is also reflected in the inability of our BSE results to demonstrate the existence of a significant fraction of low-mass He white dwarfs.

From a theoretical point of view the problem of the determination of surface gravities and masses from line spectra of HFMWDs has also proved to be insoluble, except for low-field objects ( $B \lesssim 3$  MG) for which we can assume that the magnetic field does not affect the atmospheric structure. In these objects the field broadening is negligible and standard zero-field Stark broadening theories can be used to calculate the line wings (e.g. Ferrario et al. 1998) and thus to determine the mass of the magnetic white dwarf. In principle it should also be possible to use stationary field components that are insensitive to field structure to estimate gravities from line profiles for HFMWDs. Regrettably this is not yet possible because a full theory of Stark broadening in the presence of crossed electric and magnetic fields (Main et al. 1998) has not yet been developed. For now, reliable mass determinations are only available for a few low-field magnetic white dwarfs, for magnetic white dwarfs which have good trigonometric parallaxes and magnetic white dwarfs with white dwarf companions whose atmospheric parameters can be established (e.g. RE J0317-853, Barstow et al. 1995; Fer-

**Table 9.** Known HFMDs with poloidal field strength  $B_{\text{pol}} \geq 10^5$  G. In the comparison with our models we exclude five of these white dwarfs with  $B_{\text{pol}} < 1$  MG (nos 1, 3, 18, 20 and 32) and two more of extremely low mass (nos 19 and 29) that cannot be formed within the BSE formalism.

No.	white dwarf	Aliases	$B_{\text{pol}}/\text{MG}$	$T_{\text{eff}}/\text{K}$	Mass/ $M_{\odot}$	References
1	0009+501	LHS 1038, G217-037, GR381	$\lesssim 0.2$	$6540 \pm 150$	$0.74 \pm 0.04$	1,23
2	0011-134	LHS 1044, G158-45	$16.7 \pm 0.6$	$3010 \pm 120$	$0.71 \pm 0.07$	2, 3
3	0257+080	LHS 5064, GR 476	$\approx 0.3$	$6680 \pm 150$	$0.57 \pm 0.09$	2
4	0325-857	EUVE J0317-855	185 – 450	33000	$1.34 \pm 0.03$	4
5	0503-174	LHS 1734, LP 777-001	$7.3 \pm 0.2$	$5300 \pm 120$	$0.37 \pm 0.07$	2, 3
6	0584-001	G99-37	$\approx 10$	$6070 \pm 100$	$0.69 \pm 0.02$	5,6,7
7	0553+053	G99-47	$20 \pm 3$	$5790 \pm 110$	$0.71 \pm 0.03$	2, 7, 8
8	0637+477	GD 77	$1.2 \pm 0.2$	$14870 \pm 120$	0.69	9, 10
9	0745+304	SDSS J074853.07+302543.5	11.4	$21000 \pm 2000$	$0.81 \pm 0.09$	44
10	0821-252	EUVE J0823-254	2.8 – 3.5	$43200 \pm 1000$	$1.20 \pm 0.04$	11
11	0837+199	EG 061 <sup>b</sup> , LB 393	$\approx 3$	$17100 \pm 350$	$0.817 \pm 0.032$	12
12	0912+536	G195-19	100	$7160 \pm 190$	$0.75 \pm 0.02$	2, 13, 14
13		SDSS J092646.88+132134.5	$210 \pm 25$	$9500 \pm 500$	$0.62 \pm 0.10$	15
14	0945+246	LB11146 <sup>a</sup>	670	$16000 \pm 2000$	$0.90 (+0.10, -0.14)$	16, 17
15	1026+117	LHS 2273	18	$7160 \pm 190$	0.59	18
16	1220+234	PG1220+234	3	26540	0.81	19
17	1300+590	SDSS J13033.48+590407.0	$\approx 6$	$6300 \pm 300$	$0.54 \pm 0.06$	20
18	1328+307	G165-7	0.65	$6440 \pm 210$	$0.57 \pm 0.17$	21
19	1300+015	G62-46	$7.36 \pm 0.11$	6040	0.25	22
20	1350-090	LP 907-037	$\lesssim 0.3$	$9520 \pm 140$	$0.83 \pm 0.03$	23, 24
21	1440+753	EUVE J1439+750 <sup>a</sup>	14 – 16	20000-50000	$1.04 (+0.88, -1.19)$	25
22	1503-070	GD 175 <sup>a</sup>	2.3	6990	$0.70 \pm 0.13$	2
23		SDSS J150746.80+520958.0	$65.2 \pm 0.3$	$18000 \pm 1000$	$0.99 \pm 0.05$	15
24		SDSS J150813.24+394504.0	18.9	$18000 \pm 2000$	$0.88 \pm 0.06$	44
25	1533-057	PG 1355-057	$31 \pm 3$	$20000 \pm 1040$	$0.94 \pm 0.18$	26, 27, 25
26	1639+537	GD 356, GR 329	13	$7510 \pm 210$	$0.67 \pm 0.07$	2, 28, 29, 45
27	1658+440	1658+440, FBS 376	$2.3 \pm 0.2$	$30510 \pm 200$	$1.31 \pm 0.02$	11, 30
28	1748+708	G240-72	$\gtrsim 100$	$5590 \pm 90$	$0.81 \pm 0.01$	2, 5
29	1818+126	G141-2 <sup>a</sup>	$\approx 3$	$6340 \pm 130$	$0.26 \pm 0.12$	18, 31
30	1829+547	G227-35	170 – 180	$6280 \pm 140$	$0.90 \pm 0.07$	2, 8
31	1900+705	AC +70°8247, GW +70°8247 EG 129, GL 742, LHS 3424	$320 \pm 20$	16000	$0.95 \pm 0.02$	2, 32, 33, 34, 35, 36
32	1953-011	G92-40, LTT 7879, GL 772 LP 634-001, EG 135, LHS 3501	0.1 – 0.5	$7920 \pm 200$	$0.74 \pm 0.03$	2, 37, 38
33	2010+310	GD 229, GR 333	300 – 700	16000	1.10-1.20	33, 35, 39, 40, 41, 42
34	2329+267	PG 2329+267, EG 161	$2.31 \pm 0.59$	$9400 \pm 240$	$0.61 \pm 0.16$	2, 43, 24

<sup>a</sup> Unresolved DD

<sup>b</sup> Praesepe (M44, NGC 2632)

**References:** (1) Valyavin et al. (2005); (2) Bergeron, Ruiz & Leggett (2001); (3) Bergeron, Ruiz & Leggett (1992); (4) Vennes et al. (2003); (5) Angel (1978); (6) Dufour et al. (2005); (7) Pragal & Bues (1989); (8) Putney & Jordan (1995); (9) Schmidt, Stockman, Smith (1992); (10) Giovannini et al. (1998); (11) Ferrario et al. (1998); (12) Vanlandingham et al. (2005); (13) Angel (1977); (14) Angel, Illing & Landstreet (1972); (15) Dobbie et al. (2012); (16) Glenn et al. (1994); (17) Liebert et al. (1993); (18) Bergeron, Ruiz & Leggett (1997); (19) Liebert, Bergeron & Holberg (2003); (20) Girven et al. (2010); (21) Dufour et al. (2006); (22) Bergeron, Ruiz & Leggett (1993); (23) Schmidt & Smith (1994); (24) Liebert, Bergeron, Holberg (2005); (25) Vennes et al. (1999); (26) Liebert et al. (1985); (27) Achilleos & Wickramasinghe (1989); (28) Ferrario et al. (1997); (29) Brinkworth et al. (2004); (30) Schmidt et al. (1992); (31) Greenstein (1986); (32) Wickramasinghe & Ferrario (1988); (33) Wickramasinghe & Ferrario (2000); (34) Jordan (1992); (35) Angel, Liebert & Stockman (1985); (36) Greenstein et al. (1985); (37) Maxted et al. (2000); (38) Brinkworth et al. (2005); (39) Green & Liebert (1981); (40) Schmidt, Latter & Folz (1990); (41) Schmidt et al. (1996); (42) Jordan et al. (1998); (43) Moran et al. (1998); (44) Dobbie et al. (2013). (45) Ferrario et al. (1997).

rario et al. 1997a). Currently there are 34 known magnetic white dwarfs with reasonably accurately determined masses with magnetic fields stronger than  $10^5$  G. These are listed in Table 9 with their poloidal magnetic field strengths, effective temperatures, masses and references in the literature. If we restrict ourselves to the HFMDs with  $B > 1$  MG we end up with 29 objects. When comparing with our models we exclude a further two extremely low-mass white dwarfs

because it is not possible to form these within the BSE formalism. The most recent additions to this list are the two common proper motion pairs from the SDSS reported by Dobbie et al. (2013). We shall test our hypothesis on this restricted mass sample with the caveat that we may well be still neglecting observational biases. We also note that the observational sample is neither volume nor magnitude limited.

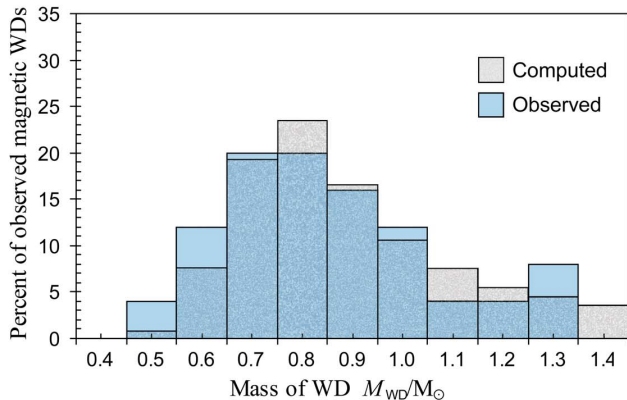


**Figure 4.** Mass distribution of 27 observed HFMWDs (objects taken from Table 9) compared with the computed sample.

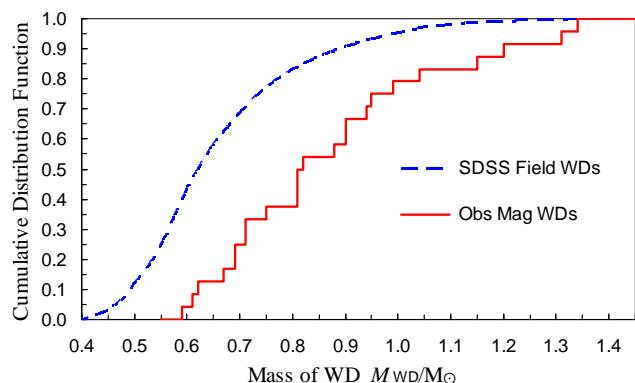


**Figure 5.** CDFs of volume-limited-converted masses of observed SDSS DR7 (Kleinman et al. 2013) non-magnetic, field white dwarfs and the observed magnetic white dwarfs. The population of observed magnetic white dwarfs is not strictly a volume limited sample since it comes from various surveys as discussed in the text. A formal application of the K–S test has  $D = 0.4417$  and  $P = 3 \times 10^{-5}$ .

The comparison of the mass distribution between theory and observations is shown in Fig. 4. Most of our models reproduce the observed peak near  $0.8 M_{\odot}$  but are less successful at reproducing the higher and lower mass tails. Interestingly the peak is dominated by giant cores that merge with main-sequence stars. This case was not considered by García-Berro et al. (2012) who focused only on merging DDs. We have used a Kolmogorov-Smirnov (K–S) test (Press et al. 1992) to compare the mass distribution of the observed HFMWDs with our synthetic populations. The K–S test determines the statistical probability that two sample sets are drawn from the same population. It uses the CDFs of the two sample sets which naturally agree at the smallest value of an independent variable where they are both zero and again at its maximum where they are both unity. The test then uses the intervening behaviour to distinguish the populations. The test gives a statistic  $D$  which is the maximum of the absolute difference between two CDFs at a given  $M_{\text{WD}}$  and the probability  $P$  that a random selection from the population would lead to a larger  $D$  than that measured.

Fig. 5 shows the mass distribution CDFs for the 27 observed HFMWDs (jagged line) and for the 12 803 SDSS DR7 field white dwarfs (smooth curve). A visual inspection shows the two CDFs to be distinctly different. The K–S test

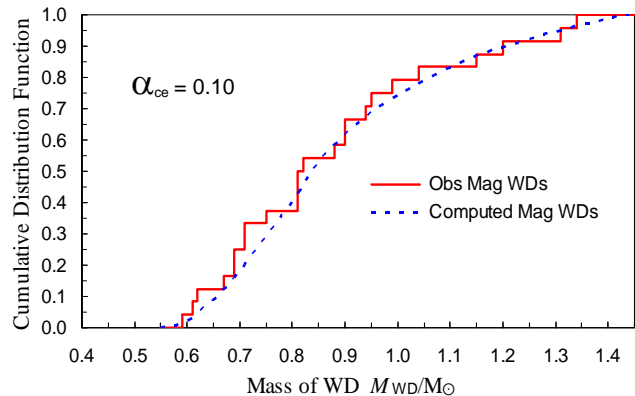


**Figure 6.** CDF of observed and BSE theoretical HFMWD masses for a Galactic disc age of 9.5 Gyr and  $\alpha = 0.10$ . The K–S test has  $D = 0.1512$  and  $P = 0.7095$ .

**Table 10.** Kolmogorov-Smirnov  $D$  statistic and  $P$  of the mass distributions of the theoretical (BSE) and observed magnetic white dwarf populations being drawn from the same distribution for various values of  $\alpha$ . The theoretical population is for a Galactic disc age of 9.5 Gyr.

$\alpha$	$D$	$P$
0.05	0.1558	0.6735
0.10	0.1512	0.7095
0.20	0.1565	0.6684
0.25	0.1616	0.6288
0.30	0.1675	0.5824
0.40	0.1827	0.4700
0.50	0.2040	0.3326
0.60	0.2304	0.2039
0.70	0.2580	0.1144
0.80	0.2814	0.0665
0.90	0.2915	0.0518

gives a  $D = 0.4417$  and  $P = 3 \times 10^{-5}$ . So we deduce that HFMWD masses are not distributed in the same manner as non-magnetic single white dwarfs. When the CDF for the observed HFMWD mass distribution is compared to the CDF for the BSE theoretical mass distribution (Fig. 6) for  $\alpha = 0.10$  it can be seen that the two curves are remarkably similar. The K–S test gives a smaller  $D$  of 0.1512 with a probability of 0.7095 that indicates success of our model. The results of the K–S test for a range of  $\alpha$ s (Table 10) show that the mass distribution is consistent over the wide range  $0.05 \leq \alpha \leq 0.7$ . On the other hand, based on the results in Table 8 the observed incidence of magnetism, as observed in the Kawka et al. (2007) volume-limited sample, constrains  $\alpha$  to be in the narrower range  $0.1 \leq \alpha \leq 0.3$ .

## 6 DISCUSSION AND CONCLUSIONS

Two competing models for the origin of strong magnetic fields in white dwarfs are broadly the fossil field model and the merging star model. The proponents of the fossil field model have noted that the maximum poloidal flux observed in the magnetic Ap and Bp stars is similar to the maximum poloidal magnetic flux observed in the magnetic white dwarfs. The two groups of stars could therefore be evolutionarily linked. However, to date, there have been no stellar

evolution models that have shown how a strong fossil magnetic flux can survive through the various stages of stellar evolution through to the white dwarf phase. It is also not clear if the similarities in the maximum magnetic fluxes between two groups of stars is necessarily a reason to assume a causal link. The dynamo model of Wickramasinghe, Tout & Ferrario (2014) suggests that similar maximum magnetic fluxes may be expected for physical reasons if the fields are generated from differential rotation caused by merging. Here we have explored the consequences of such a hypothesis for the origin of the HFMWDs with binary population synthesis under standard assumptions, discussed in section 3. We have found the following.

- (i) While the mass distribution of HFMWDs is not very sensitive to  $\alpha$ , good agreement can be obtained with both the observed mass distribution and the observed incidence of magnetism for models with  $0.1 \leq \alpha \leq 0.3$ . In particular the mean predicted mass of HFMWDs is  $0.88 M_{\odot}$  compared with  $0.64 M_{\odot}$  (corrected to include observational biases) for all white dwarfs while observations indicate respective mean masses of  $0.85 M_{\odot}$  (see also Kepler et al. 2013) and  $0.62 M_{\odot}$  (Kleinman et al. 2013). A K-S test shows that the small number of reliably measured masses of HFMWDs are not distributed in the same way as the masses of non-magnetic single white dwarfs. The probability they are is only  $3 \times 10^{-5}$ . On the other hand our best model fit to the observed mass distribution of HFMWDs has a probability of 0.71.
- (ii) Stars that merge during common envelope evolution and then evolve to become white dwarfs outnumber merging post-common envelope DD systems for all  $\alpha$ . The common envelopes yield mainly CO white dwarfs with a few He and ONe white dwarfs, while the DDs yield only CO white dwarfs.
- (iii) The major contribution to the observed population of HFMWDs comes from main-sequence stars merging with degenerate cores at the end of common envelope evolution. The resulting giants go on to evolve to HFMWDs.
- (iv) The merging DDs tend mostly to populate the high-mass end of the white dwarf mass distribution.

We also note that the study by Zorotovic et al. (2010) of the evolution of a sample of SDSS post-common envelope binary stars consisting of a white dwarf and a main-sequence star indicates that the best agreement with observational data is achieved when  $\alpha = 0.25$  and this is consistent with our findings.

In summary, available observations of the mass distribution and incidence of HFMWDs are compatible with the hypothesis that they arise from stars that merge mostly during common envelope evolution with a few that merge during post-common envelope evolution as DD systems. Our calculations, when taken together with the observation that there are no examples of HFMWDs in wide binary systems, allow us to argue strongly in favour of this hypothesis. In the majority of cases the fields may be generated by a dynamo mechanism of the type recently proposed by Wickramasinghe, Tout & Ferrario (2014). The disc field model of Nordhaus et al. (2011) or the model proposed by García-Berro et al. (2012) may be relevant in the case of merging DD cores depending on mass ratio. The rate of merging of post-common envelope DDs alone is too low to account for all observed HFMWDs.

## ACKNOWLEDGEMENTS

We would like to thank the Referee, Zhanwen Han, for his suggestions and comments which have helped us improving the quality of this paper. GPB gratefully acknowledges receipt of an Australian Postgraduate Award. CAT thanks the Australian National University for supporting a visit as a Research Visitor of its Mathematical Sciences Institute, Monash University for support as a Kevin Watford distinguished visitor and Churchill College for his fellowship.

## REFERENCES

- Achilleos N., Wickramasinghe D. T., 1989, *ApJ*, 346, 444
- Angel J. R. P. 1977, *ApJ*, 216, 1
- Angel J. R. P. 1978, *ARA&A*, 16, 487
- Angel J. R. P., Illing R. M. E., Landstreet J. D., 1972, *ApJ*, 175, L85
- Angel J. R. P., Liebert J., Stockman H. S., 1985, *ApJ*, 292, 260
- Barstow M.A., Jordan S., O'Donoghue D., Burleigh M. R., Napiwotzki R., Harrop-Allin M.K., 1995, *MNRAS*, 277, 971
- Bergeron P., Leggett S. K., Ruiz M. T., 2001, *ApJS*, 133, 413
- Bergeron P., Ruiz M. T., Leggett S. K., 1992, *ApJ*, 400, 315
- Bergeron P., Ruiz M. T., Leggett S. K., 1993, *ApJ*, 407, 733
- Bergeron P., Ruiz M. T., Leggett S. K., 1997, *ApJS*, 108, 339
- Bisnovatyi-Kogan G. S., Sunyaev R. A., 1971, *Astron. Zh.*, 48, 881
- Brinkworth C. S., Burleigh M. R., Wynn G. A., Marsh T. R., 2004, *MNRAS*, 348, L33
- Brinkworth C. S., Marsh T. R., Morales-Rueda L., Maxted P. F. L., Burleigh M. R., Good S. A., 2005, *MNRAS*, 357, 333
- de Kool M., 1990, *ApJ*, 358, 189
- Dobbie P. D., Baxter R., Külebi B., Parker Q. A., Koester D., Jordan S., Lodieu N., Euchner F., 2012, *MNRAS*, 421, 202
- Dobbie P. D. et al., 2013, *MNRAS*, 428, L16
- Dufour P., Bergeron P., Fontaine G., 2005, *ApJ*, 627, 404
- Dufour P., Bergeron P., Schmidt G. D., Liebert James., Harris H. C., Knapp G. R., Anderson S. F., Schneider D. P., 2006, *ApJ*, 651, 1112
- Ferrario L., Wickramasinghe D. T., Liebert J., Schmidt G. D., Biegging J. H., 1997a, *MNRAS*, 289, 105
- Ferrario L., Vennes S., Wickramasinghe D. T., Bailey J., Christian D. J., 1997b, *MNRAS*, 292, 205
- Ferrario L., Vennes S., Wickramasinghe D. T., 1998, *MNRAS*, 299, L1
- Ferrario L., Pringle J. E., Tout C. A., Wickramasinghe D. T. 2009, *MNRAS*, 400, L71
- Ferrario L. 2012, *MNRAS*, 426, 2500
- García-Berro E. et al., 2012, *ApJ*, 749, 25
- Giovannini O., Kepler S. O., Kanaan A., Wood M. A., Claver C. F., Koester D., 1998, *Baltic Astron.*, 7, 131
- Girven J., Gänsicke B. T., Külebi B., Steeghs D., Jordan S., Marsh T. R., Koester D., 2010, *MNRAS*, 404, 159

- Glenn J., Liebert J., Schmidt, G. D., 1994, *PASP*, 106, 722
- Green R. F., Liebert J., 1981, *PASP*, 93, 105
- Greenstein J. L., 1986, *ApJ*, 304, 334
- Greenstein J. L., Henry R. J. W., O'Connell R. F., 1985, *ApJ*, 289, L25
- Han, Z.; Podsiadlowski, P.; Eggleton, P. P., *MNRAS*, 270,121
- Han, Z.; Podsiadlowski, Ph.; Maxted, P. F. L.; Marsh, T. R.; Ivanova, N. *MNRAS*, 336, 449
- Hurley J. R., Pols O.R., Tout C. A., 2000, *MNRAS*, 315, 543
- Hurley J. R., Tout C. A., Pols O. R., 2002, *MNRAS*, 329, 897
- Jordan S., 1992, *A&A*, 265, 570
- Jordan S., Schmelcher P., Becken W., Schweizer W., 1998, *A&A*, 336, L33
- Kawka A., Vennes S., Schmidt G. D., Wickramasinghe D. T., Koch R., 2007, *ApJ*, 654, 499
- Kepler S.O. et al., 2013, 429, 2934
- Kleinman S. J. et al., 2013, *ApJS*, 204, 5
- Landstreet J. D., Bagnulo S., Valyavin G. G., Fossati L., Jordan S., Monin D., Wade G. A., 2012, *A&A*, 545, A30
- Liebert J., 1988, *PASP*, 100, 1302
- Liebert J., Bergeron P., Schmidt G. D., Saffer R. A., 1993, *ApJ*, 418, 426
- Liebert J., Bergeron P., Holberg J.B., 2003, *AJ*, 125, 348
- Liebert J., Bergeron P., Holberg J. B., 2005, *ApJS*, 156, 47
- Liebert J., Schmidt G. D., Sion E. M., Starrfield S. G., Green R. F., Boroson T. A., 1985, *PASP*, 97, 158
- Liebert J. et al., 2005a, *AJ*, 129, 2376
- Liu W. M., Chaboyer B., 2000, *ApJ*, 544, 818
- Livio M., Soker N., 1988, *ApJ*, 329, 764
- Mestel L., Landstreet J. D., 2005, in Wielebinski R., Beck R., eds, *Cosmic Magnetic Fields*. Springer-Verlag, Berlin, p. 183
- Main J., Schwacke M., Wunner G., 1998, *Phys. Rev. A*, 57, 1149-1
- Maxted P. F. L., Ferrario L., Marsh T. R., Wickramasinghe D. T., 2000, *MNRAS*, 315, L41
- Meng X., Chen X., Han Z. 2008, *A&A*, 487,625
- Moran C., Marsh T. R., Dhillon V. S., 1998, *MNRAS*, 299, 218
- Nordhaus J., Wellons S., Spiegel D. S., Metzger B. D., Blackman E. G., 2011, *Proc. Natl Acad. Sci.*, 108, 3135
- Oswalt T. D., Smith J. A., Wood M. A., Hintzen P., 1996, *Nature*, 382, 692
- Potter A. T., Tout C. A., 2010, *MNRAS*, 402,1072
- Potter A. T., Chitre S. M., Tout C. A., 2012, *MNRAS*, 424, 2358
- Power J., Wade G. A., Aurière M., Silvester J., Hanes D., 2008, *Contrib. Astron. Obs. Skalnaté Pleso*, 38, 443
- Pragal M., Bues I., 1989, *Astron. Ges. Abstr. Ser.*, 2, 45
- Press W. H., Teukolsky S. A., Vetterling W. T., Flannery B. P., 1992, *Numerical Recipes in Fortran 77. The Art of Scientific Computing*, Cambridge Univ. Press, Cambridge
- Putney A., Jordan S., 1995, *ApJ*, 449, 863
- Salpeter E. E., 1955, *ApJ*, 121, 161
- Schmidt G. D., Allen R. G., Smith P. S., Liebert J., 1996, *ApJ*, 463, 320
- Schmidt G. D., Bergeron P., Liebert J., Saffer R. A., 1992, *ApJ*, 394, 603
- Schmidt G. D., Latter W. B., Foltz C. B., 1990, *ApJ*, 350, 758
- Schmidt G. D., Smith P. S., 1994, *ApJ*, 423, L63
- Schmidt G. D., Stockman H. S., Smith P. S., 1992a, *ApJ*, 398, L57
- Tauris T. M., Dewi J. D. M., 2001, *A&A*, 369, 170
- Tout C. A., Wickramasinghe D. T., Liebert J., Ferrario L., Pringle J. E., 2008, *MNRAS*, 387, 897
- Valyavin G., Bagnulo S., Monin D., Fabrika S., Lee B. C., Galazutdinov G., Wade G. A., Burlakova T., 2005, *A&A*, 439, 1099
- van den Heuvel E. P. J., 1976, in Eggleton P., Mitton S., Whelan J., eds, *Proc. IAU Symp. 73, Structure and Evolution of Close Binary Systems*. Reidel, Dordrecht, p. 35
- Vanlandingham K. M. et al., 2005, *AJ*, 130, 734
- Vennes S., Ferrario L., Wickramasinghe D. T., 1999, *MNRAS*, 302, L49
- Vennes S., Schmidt G. D., Ferrario L., Christian D. J., Wickramasinghe D. T., Kawka A., 2003, *ApJ*, 593, 1040
- Wickramasinghe D. T., Ferrario L., 1988, *ApJ*, 327, 222
- Wickramasinghe D. T., Ferrario L., 2000, *PASP*, 112, 873
- Wickramasinghe D. T., Ferrario L., 2005, *MNRAS*, 356, 615
- Wickramasinghe D. T., Tout C. A., Ferrario L., 2014, *MNRAS*, 437, 675
- Zorotovic M., Schreiber M. R., Gänsicke B. T., Nebot Gómez-Morán A., 2010, *A&A*, 520, 86